

Spectral and Time Resolved Measurements of Pollutants on Water Surface by a XeCl Laser Fluorosensor

R. Barbini, R. Fantoni, A. Palucci*, S. Ribezzo and H.J.L.van der Steen

ENEA, Dip. Sviluppo Tecnologie di Punta, CRE Frascati
P.O. Box 65, 08044 Frascati (RM), Italy

*ENEA guest

ABSTRACT

An excimer laser based LIDAR fluorosensor, designed for operation from a mobile station, has been assembled at the ENEA Centre in Frascati and laboratory measurements on different samples have been performed both with spectral and time resolution. A low divergence high power XeCl laser has been used for excitation of typical chemical and biological materials polluting water surfaces. Results obtained on thin films of oils most frequently found in the Mediterranean sea.

A rough correlation has been found connecting the average oil density with both the overall visible fluorescence yield as well as the time decay constants. Lighter oils have shown more intense bands with longer time decay constants respect to heavier oils.

INTRODUCTION

The increasing interest in environmental problems during the last years has pushed scientists towards the development of detection systems, suitable for monitoring ecological equilibria over a wide range and for detecting the presence of hazardous species. High power laser sources in the visible and the u.v. are the basis of active LIDAR instruments. The early development of visible laser sources such as solid state lasers (Ruby, Nd:YAG doubled) and noble gas discharge lasers (HeNe, Ar⁺, Kr⁺) allowed scientists to consider the possible detection of major pollutants in the environment either through Raman scattering or through fluorescence signals which, for most of the organic materials, fall in the visible spectrum. In the last ten years, airborne measurements (Hoge & Swift, 1980; O'Neil, 1980) of Raman and fluorescence signals were carried out mostly by using available near u.v. laser sources, such as the N₂ laser, emitting at 337 nm, or the triplicated Nd:YAG laser, emitting at 355 nm. Both these standard sources are characterized by a pulse duration around 10 ns with either relatively low energy (1 to 10 mJ)

and high repetition rate (100 to 500 Hz) (N₂ laser), or with a higher energy (10 to 100 mJ) but a lower repetition rate (1 to 10 Hz) (III harmonic Nd:YAG laser).

The use of near U.V. lasers sources introduces several advantages with respect to visible sources since most of the organic substances, especially those containing aromatic rings or conjugated chains of double and triple bonds, can be effectively excited in the near u.v. and respond with a rather strong fluorescence. This signal, after proper spectral and time analysis, constitutes a finger-print of the molecule or, at least, of the kind of molecules involved in the excitation process.

On the other hand, the possibility of detecting a lot of different species by recognizing their fluorescence emission bands or by vibrational Raman scattering, can render the visible spectrum quite crowded. But the recent development of large intensified Optical Multichannel Analysers (OMA), together with the use of excitation sources emitting more towards the u.v., has made the detection of high resolution spectral and time decay signals much easier. Nowadays, commercial pulsed excimer lasers are available with high output energy (100 to 200 mJ), high repetition rate (100 to 200 Hz), relatively short pulses (10 to 20 ns) and a controlled divergence. Taking into account the ν dependence of the Raman cross section, the atmospheric windows and the excitation efficiency of the species under investigation, a reasonable compromise can be found for the excitation source. For instance, a good choice is represented by the XeCl excimer laser emitting at 308 nm with high energy output and good stability. At this wavelength, the atmospheric transmission is close to its maximum and open sea water is sufficiently transparent to allow for measurements up to 50 m below the sea surface.

The present paper deals with measurements of oil pollution on the sea surface. A typical spectrum of polluted sea water will contain, apart from the backscattered XeCl radiation at 308 nm, the intense water Raman signal at

≈ 344 nm (with a Raman shift of ≈ 3300 cm^{-1} due to the OH stretching), the 'gelbstoff' fluorescence from organic and biological wastes, which is peaked between 400 nm and 410 nm, the fluorescence of light and heavy oils peaked respectively around 450 nm and 500 nm, and some chlorophyll contributions peaked around 685 nm due to vegetation just below the sea level.

In section 1 the XeCl excimer laser based LIDAR fluorosensor built at the ENEA Centre in Frascati will be described in the configuration for both spectral and time resolved measurements. Laboratory results obtained on different middle-east crude oils are discussed in section 2, where both direct fluorescence measurements (section 2.1) and water Raman signals (section 2.2) are reported. Results of time resolved measurements are shown and discussed in section 2.3.

1. EXPERIMENTAL SET-UP

The prototype laboratory set-up to be assembled in an airborne configuration is sketched in fig. 1. A narrowband high power excimer laser (EMG 1003i, Lambda Physik) provides a low divergence beam at 308 nm. After following a long optical path, necessary for compensating intrinsic instrumental delay times, the laser radiation reaches (with a spotsize of approximately 10×10 cm^2) the sample holder, which is a deep basin containing the oil either at the bottom or on the surface of a water column.

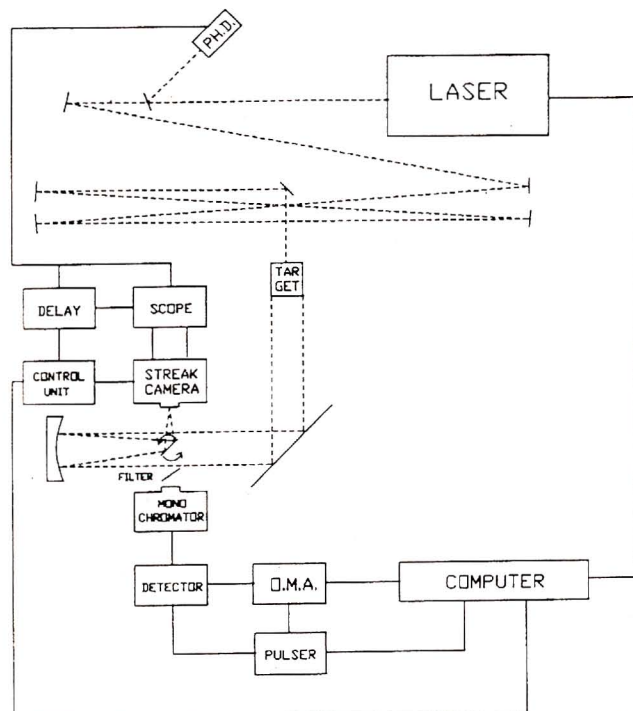


Fig. 1 - Laboratory experimental set-up for fluorosensor LIDAR.

The fluorescence signal is detected either on a fast Streak Camera, for time resolved measurements, or on the OMA detector in the case of spectrally resolved measurements, after passing a monochromator and, if necessary, a filter for removing the backscattered fraction of the excitation wavelength. When doing time resolved measurements, a controllable delay unit triggered by the signal generated by a fast photodiode is added, in order to set the streak camera time window. By incrementing the delay time orderly we get a number of files which can be assembled by the controlling computer. In this way a large time window together with the high time resolution of the streak camera can be obtained. Both for OMA and streak camera, an average is made over a number of pulses: because of this, the effective repetition rate is up to 30 Hz. The available computer (IBM PC/AT) is used to control the OMA together with the laser and the streak camera, and is further dedicated to do both data acquisition and data analysis. The main characteristics of this experimental set-up are listed in Tab.I.

TABLE 1

Main characteristics of the experimental set-up

Laser:	XeCl excimer laser
Lambda	Positive branch
Physics	unstable cavity
EMG 1003i	Emission wavelength 308 nm
	Pulse energy typically 150 mJ
	Pulse width 17 ns (3 long. modes)
	P.R.R. max. 200 Hz
	divergence (θ) hor. 0.4 mrad
	ver. 0.2 mrad
Receiver:	Newtonian telescope d=20 cm
	f#5
Data acquisition system:	
O.M.A.III:	Intensified photodiode
EG&G	array detector 1421
	Pulse amplifier 1304
	Fast pulser 1302
	HR-320 monochromator 0.32 m
	Spectral channels 1024
	Spectral resolution 5 Å (147 g/mm)
	0.3 Å (1800 g/mm)
Streak	2491 control unit
Camera:	C2830 temporal disperser
	Temporal ranges 0.5, 1, 2, 5, 10 ns
Hamamatsu	Temporal channels 512
	Temporal resolution 10 ps or better

2. RESULTS AND DISCUSSION

2.1 Fluorescence spectra of oils

A typical fluorescence spectrum from a water column is reported in Fig. 2., the water Raman peak is revealed at 344 nm followed by the broad gelbstoff fluorescence in the blue region.

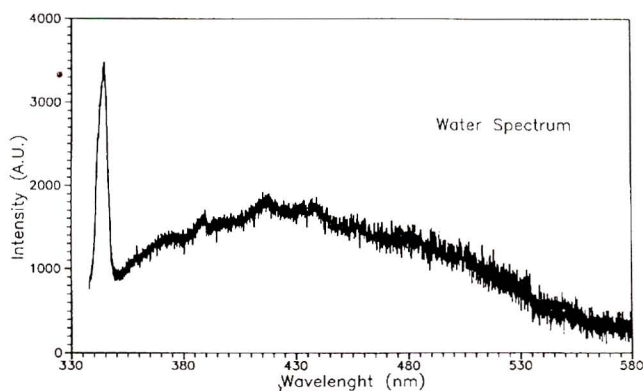


Fig. 2 - Raman and fluorescence spectrum of water excited at 308 nm.

Four different crude oil samples of Middle East origin have been considered for the present laboratory experiments. Their average bulk density has been measured together with their absorptivity in the near u.v. region (from 300 nm to 400 nm). Due to the very large absorption by oils in this range, u.v. absorbance has been measured in diluted trichloroethylene solutions (10^{-4} to 10^{-3} g/cm³) by means of a double beam u.v. spectrophotometer (Perkin Elmer mod. 330). Oil density and absorptivity at a few wavelengths of interest are reported in table 2. Under the rather crude assumption that solvation affects in the same way the u.v. absorption spectra of the four different oils, bulk extinction coefficients can be obtained from the measured absorptivity. Extinction coefficients, also reported in Table 2, have been obtained after normalization with the value at 344 nm from the data for Kirkuk oil measured by Bertolini, 1988 and Camagni, 1988.

TABLE 2

Physical and optical properties of some crude oil samples of Middle East origin. A=measured absorptance, b=optical path length (0.2 cm, 1.0 cm), c=oil concentration: $a=A/(b \cdot c)$. Measurements have been performed diluting the oils in trichloroethylene, with typical concentrations in the range 0.0001 - 0.001 g/cm³. Uncertainty on density is 0.02 g/cm³, on absorptivity about 20%.

Oil	density (g/cm ³)	w.l. (nm)	absorptivity a (cm ² /g)	extinct. coef. k (nm)
Kirkuk	0.85	308	848	1.10*
		344	495	0.64*
		362	384	0.50
Iranian Light	0.87	308	231	0.30
		344	172	0.22
		362	131	0.17
Zarzaitine	0.84	308	288	0.37
		344	134	0.17
		362	106	0.14
Saharan Blend	0.81	308	319	0.41
		344	136	0.18
		362	103	0.13

*. Samples supplied by Stazione Sperimentale per i Combustibili (S. Donato Milanese).

#. Interpolated from reference (Camagni, 1988) values measured at 337 nm and 355 nm on undiluted samples. This value has been used for renormalization of present absorptivity data.

From Table 2 we observe that heavier oils, like Kirkuk, have a higher absorptivity in the near u.v. In spite of this, heavy oils usually present a low fluorescence yield after near u.v. excitation (Bertolini, 1988; Camagni, 1988). Large differences, over more than one order of magnitude, in absolute fluorescence yields have been already observed between light and heavy oils (Hoge, 1983; Visser, 1979).

On the other hand, only small differences in spectral shape have been detected in the case of oil fluorescence (Bertolini, 1988; Camagni, 1988). This is confirmed by the present experimental data on our four samples with different densities. Measurements have been performed first at low resolution, by placing a filter in front of the OMA for removing all wavelengths smaller than 360 nm (i.e. mostly the backscattered laser radiation at 308 nm and the water Raman signal at 344 nm). Spectra of arbitrary thick oil films on a water column are shown in Fig. 3. Fluorescence emission covers most of the visible spectral range. Spectral shapes are quite similar throughout this region, where three maxima can be identified, roughly peaked at 460 nm, 490 nm and 540 nm, respectively.

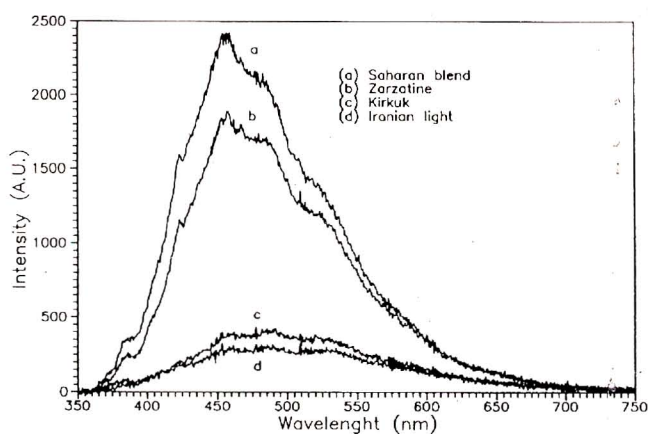


Fig. 3 - Fluorescence spectra of four different crude oil samples.

Our measurements (not shown) repeated at higher resolution did not reveal the presence of any sharper feature, only shoulders in the near U.V. region at 360 nm, 390 nm and 440 nm became more evident because the U.V. filter was not used in combination with the high resolution grating. The general trend shown by spectral shapes is a broadening of the fluorescence spectra towards longer wavelengths with increasing oil density.

In conclusion, the presence of oils on a water surface can be recognized from their typical emission spectra, but the direct identification of the specific oil seems to be rather

difficult if no additional information, e.g. the time decay constants at different wavelength as discussed in sect. 2.3, is available.

2.2 Measurements of water Raman signal

The O-H stretching in water is Raman active with a Stokes shift of 3300 cm^{-1} . Illumination of a water column by means of a 308 nm laser radiation gives rise to the water Raman signal centered at 344 nm . In (Leonard, 1979) it has been demonstrated that the peculiar shape of the liquid water Raman peak is traceable to the contemporary presence of monomers and molecular aggregates, so that it is sensitive to temperature which affects the respective equilibrium. In our laboratory, measurements of the water Raman signal have been performed at high resolution in the range 330 nm to 365 nm in order to discriminate from the intense tail of the backscattered laser radiation. First the linearity of the Raman response from clean (without oil) water has been checked vs the the water column height. After background subtraction, the integrated intensity under the water peak (between 340 nm and 348 nm) turned out to increase linearly with the water column height.

Measurements in the same wavelength range have been performed after adding fixed amounts (drops) of different oils on the surface above a certain water column. Selected spectra are shown in Fig. 4, for Kirkuk and Saharan Blend oil. Results (not shown) for Iranian Light and Zarzaitine were rather similar to the first and the second of the former samples. In Fig. 4 we first notice that the water Raman peak is progressively depressed by the oil absorption of 308 nm laser radiation which thus cannot effectively penetrate in the water column. We also detect in this range (around 360 nm) the first peak of the oil fluorescence spectrum, which is especially intense in the case of the lightest oil (Saharan Blend). On the other hand, and possibly due to the low thickness of the oil samples over the water surface (each drop contains less than 0.02 g of oil spread over about 600 cm^2), no Raman signal related to C-H stretchings in oils (Raman shifts between $2900\div 3200\text{ cm}^{-1}$) is detected in the range $338\div 341\text{ nm}$.

In order to use the LIDAR fluorosensor for field measurements of oil film thickness on sea water, the dependence of oil fluorescence intensity and water Raman intensity upon oil (quantity) thickness has been checked. However the integrated oil fluorescence in the range 360 to 364 nm , after proper background subtraction, vs the quantity (drops) of oil spilled upon the water surface followed a

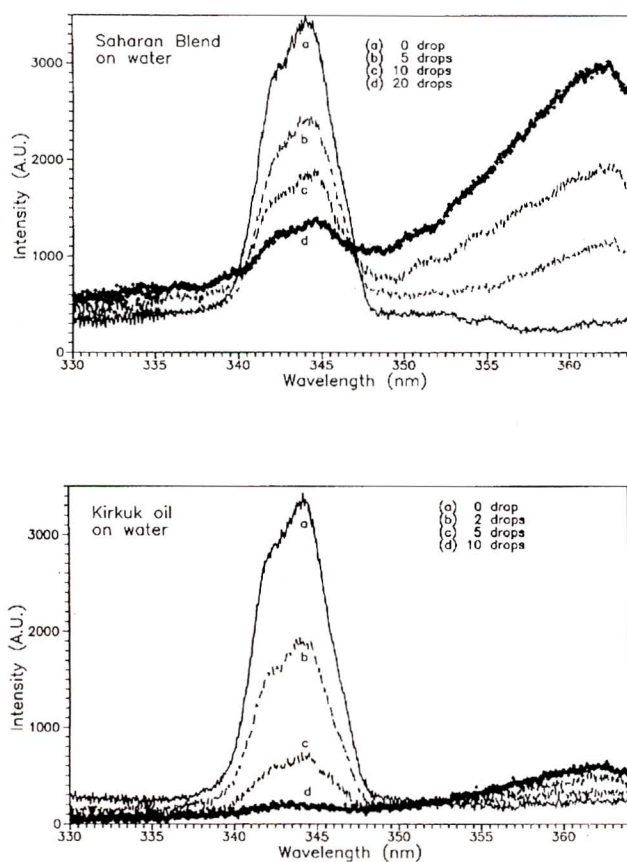


Fig. 4 - Fluorescence response and water Raman signal measured in the near u.v. as a function of the oil quantity on the water surface for two different crude oil samples.

linear behaviour only at very small quantities and reached saturation, especially for the heaviest oils. This demonstrates that absolute fluorescence measurements, which also require the knowledge of the kind of oil detected, are not suitable to determine the thickness of the pollutant film.

On the other hand, in data analysis we have observed that the integrated water Raman signal tends to follow an exponential decay law as the oil quantity on the water surface increases. By using the integrated Raman signal R_{in} measured as a function of the oil quantity and the corresponding Raman signal from clean water R_{out} , the oil thickness d can be obtained from the expression (Hoge & Kincaid, 1980; Kung, 1976):

$$d = -\frac{1}{k_e + k_R} \ln(R_{in}/R_{out})$$

where k_e and k_R are the extinction coefficients listed in table 2 at 308 nm and 344 nm , respectively.

Results for Kirkuk and Saharan Blend oil correspond to a thickness of $0.22\text{ }\mu\text{m/drop}$ and of $0.17\text{ }\mu\text{m/drop}$, respec-

tively. The ratio in thickness from the measured Raman intensities is in agreement with the ratio of weights of the respective oil drops, also taking into account the small differences in oil density. As shown in Fig. 5, the model we used is quite satisfactory and the Raman intensity plotted vs the oil thickness d is well fitted by an exponential decay for both Hirkuk and Saharan Blend oil. However, it has to be mentioned that the model could not be properly applied to the Zarzaitine and Iranian Light oil samples, because there were problems in uniformly spreading drops on the water surface.

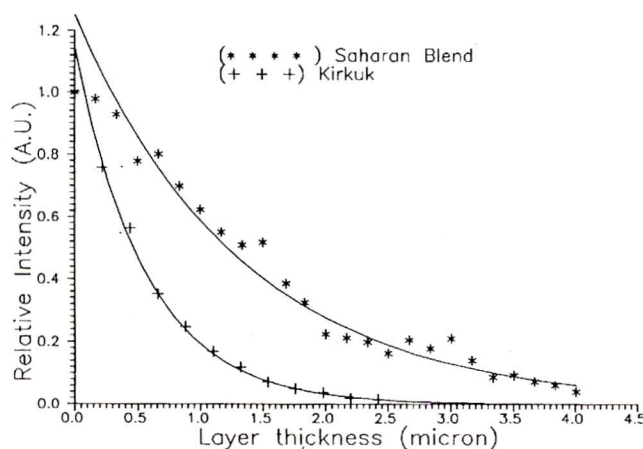


Fig. 5 - Exponential behaviour of the Raman intensity versus oil layer thickness measured for Kirkuk and Saharan Blend oils.

2.3 Time decay of oil fluorescence

Time decays curves for the four crude oil samples have been measured by using the fast streak camera with the longest time sweep (10 ns). Different parts of the excitation and decay curve have been acquired as a function of the delay counted from the laser pulse rising edge (detected with the fast photodiode, see fig. 1). At each selected delay time, 5 waveforms have been averaged. The complete curve of fluorescence intensity vs time was successively reconstructed by software.

Measurements performed without filters in front of the streak camera were dominated by the backscattered laser radiation and revealed the typical profile, shown in Fig. 6, with the three longitudinal modes of the laser pulses provided by our unstable resonator cavity. Oil fluorescence has been detected by placing an interference filter, peaked at 450 nm with a 60 nm bandwidth, in front of the streak camera entrance.

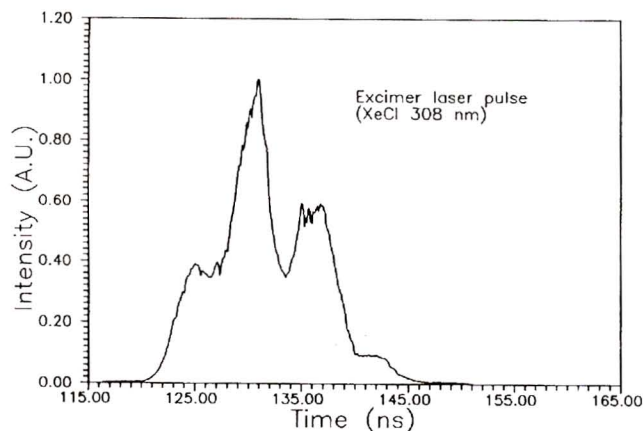


Fig. 6 - Temporal shape of typical XeCl laser pulse as measured with the streak Camera.

The fluorescence of the four crude oil samples, together with a convolution of the laser pulse (Fig. 6) with an exponential function, is shown in Fig. 7.

The values for the decay time have been obtained by fitting the fluorescence with this convolution and minimizing the chi-square difference. For both Hirkuk and Iranian Light a decay time of 2.7 ns is found, whereas Zarzaitine and Saharan Blend have decay times of 4.7 and 4.3 ns respectively. The error in each value is in the order of 0.1 ns. The observed trend in lifetime seems to be significant to the identification of the oil sample and consistent with the results reported in ref. 2. as measured after excitation at 355 nm.

Thus, as hypothesized in (Rayner, 1978) long time ago, we can conclude that measuring accurately time decay constants, together with the fluorescence spectra, should allow for the unambiguous identification of the pollutant oil in remote sensing experiments.

From the present results, it comes out that a short U.V. laser source is required for accurate time resolved oil fluorescence measurements. In our laboratory different methods for shortening the XeCl laser pulse have been considered, the best results up to now being obtained by using a Raman shifter in CH_4 . By inducing the stimulated Raman scattering at threshold for the second Stokes and laser pulses of about 1 mJ energy, 2 ns duration were generated at 378 nm. Work is in progress to excite the oil fluorescence with this radiation.

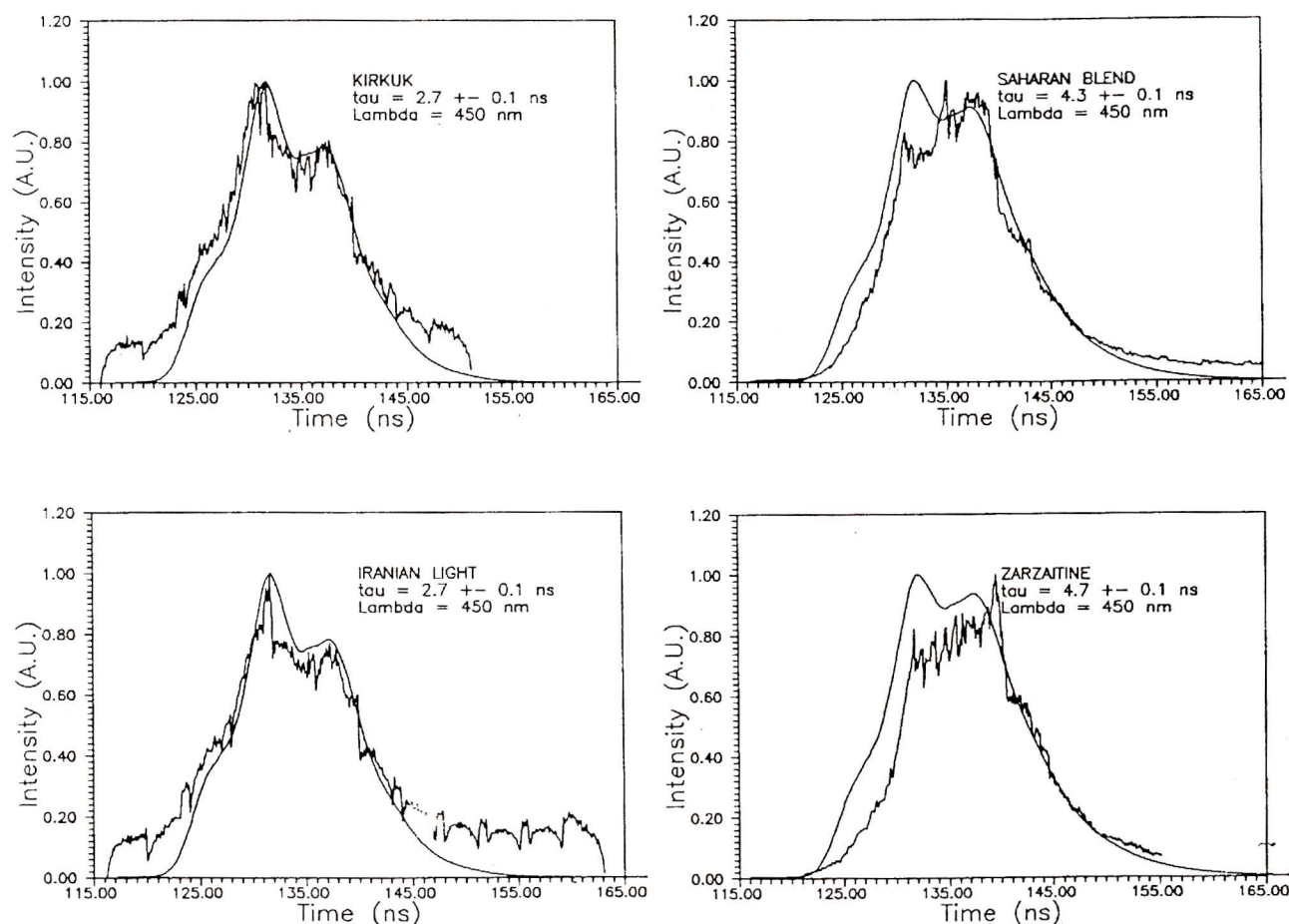


Fig. 7 - Fits of the four crude oil fluorescence signals with convolution of the exciting laser profile with an exponential function.

ACKNOWLEDGMENTS

Thanks are due to dr. F. Colao for helping in computer control of the experiment.

REFERENCES

- Bertolini G., Camagni P., Koechler C., Pedrini A. & Prosdociami A., 1988, Time-resolved laser fluorosensing: trends and applications, Proceedings of the 4th International Colloquium on Spectral signatures of Objects in Remote sensing, Aussois, France, 18-22 Jan 1988, pp.233-238.
- Camagni P., Colombo G., Koechler C., Omenetto N., Pedrini A., Rossi G., 1988, Remote characterization of mineral oils by laser fluorosensing: basic diagnostics and simulation experiments, Commission of the European Communities, Ispra Est., Report EUR 11781 EN.
- Hoge F. E. & Kincaid J. S., 1980, Laser measurements of extinction coefficients of highly absorbing liquids, Appl. Opt. 19, 1143.
- Hoge F. E. & Swift R.N., 1980, Water depth measurements using an airborne pulsed Neon laser system, Appl. Opt. 19, 3269.
- Hoge F. E. & Swift R.N., 1983, Experimental feasibility of the airborne measurements of absolute oil fluorescence spectral conversion efficiency, Appl. Opt. 22, 37.
- Kung R.T.V. & Itzkan I., 1976, Absolute oil fluorescence conversion efficiency, Appl. Opt. 15, 409.
- Leonard D.A., Caputo B. & Hoge F.E., 1979, Remote sensing of subsurface water temperature by Raman scattering, Appl. Opt. 18, 1732.
- O'Neil R.A., Buja-Bijunas L. & Rayner D.M., Field performance of a laser fluorosensor for the detection of oil spills, 1980, Appl. Opt. 19, 863.
- Rayner D.M. & Szabo A.G., 1978, Time-resolved laser fluorosensors: a laboratory study of their potential in the remote characterization of oil, Appl. Opt. 17, 1624.
- Visser H., 1979, Teledetection of the thickness of oil films on polluted water based on the oil fluorescence properties, Appl. Opt. 18, 1746.